Experimental investigation of CO_2–brine–rock interactions at elevated temperature and pressure: Implications for CO_2 sequestration in deep-saline aquifers

Robert J. Rosenbauer[*], Tamer Koksalan, James L. Palandri

U.S. Geological Survey, 345 Middlefield Road, Menlo Park, CA 94025, United States

Abstract

Deep-saline aquifers are potential repositories for excess CO_2, currently being emitted to the atmosphere from anthropogenic activities, but the reactivity of supercritical CO_2 with host aquifer fluids and formation minerals needs to be understood. Experiments reacting supercritical CO_2 with natural and synthetic brines in the presence and absence of limestone and plagioclase-rich arkosic sandstone showed that the reaction of CO_2-saturated brine with limestone results in compositional, mineralogical, and porosity changes in the aquifer fluid and rock that are dependent on initial brine composition, especially dissolved calcium and sulfate. Experiments reacting CO_2-saturated, low-sulfate brine with limestone dissolved 10% of the original calcite and increased rock porosity by 2.6%. Experiments reacting high-sulfate brine with limestone, both in the presence and absence of supercritical CO_2, were characterized by the precipitation of anhydrite, dolomitization of the limestone, and a final decrease in porosity of 4.5%. However, based on favorable initial porosity changes of about 15% due to the dissolution of calcite, the combination of CO_2 co-injection with other mitigation strategies might help alleviate some of the well-bore scale and formation-plugging problems near the injection zone of a brine disposal well in Paradox Valley, Colorado, as well as provide a repository for CO_2.

Experiments showed that the solubility of CO_2 is enhanced in brine in the presence of limestone by 9% at 25 °C and 6% at 120 °C and 200 bar relative to the brine itself. The solubility of CO_2 is enhanced also in brine in the presence of arkosic sandstone by 5% at 120 °C and 300 bar. The storage of CO_2 in limestone aquifers is limited to only ionic and hydraulic trapping. However, brine reacted

---

* Corresponding author.
  E-mail address: brosenbauer@usgs.gov (R.J. Rosenbauer).

with supercritical CO_2 and arkose yielded fixation and sequestration of CO_2 in carbonate mineral phases. Brine desiccation was observed in all experiments containing a discrete CO_2 phase, promoting porosity-reducing precipitation reactions in aquifers near saturation with mineral phases. Published by Elsevier B.V.

1. Introduction

The burning of fossil fuels has caused a continuous and dramatic 30% increase of atmospheric carbon dioxide (CO_2) over the past 150 years [1,2]. The role of CO_2 as a greenhouse gas and its potential effect on global climate have been well documented [3–5]. CO_2 sequestration in geologic formations is increasingly being studied as a strategy for limiting these anthropogenic CO_2 emissions. The disposal of CO_2 into deep-saline aquifers is one of several possible storage repositories, but the details of the geochemical reactions between supercritical CO_2 and potential host fluids and formation rocks need to be understood before pursuing this option.

Carbon dioxide reacts with water to produce carbonic acid (Eq. (1)), a fundamentally important reaction because the aqueous, not the molecular, form of CO_2 is reactive toward the aquifer rocks:

$$CO_2 + H_2O \leftrightarrow H_2CO_3 \tag{1}$$

The aqueous solubility of CO_2 is temperature-, pressure-, and ionic strength-dependent, generally lower at elevated temperature and salinity and greater at elevated pressure [6–8] At 25 °C and 1 bar, the solubility of CO_2 in an aquifer fluid equivalent to a 4 m NaCl solution is approximately one-third its solubility in pure water [6]. At down-hole disposal conditions of 120 °C and 300 bar, the solubility of CO_2 in a 4 m NaCl equivalent aquifer fluid is 0.5 m [6,7]. In the absence of any fluid or wallrock interaction, this dissolved CO_2 results in an acidic solution of pH 3.4 due to the dissociation of carbonic acid (Eq. (2)):

$$H_2CO_3 \leftrightarrow H^+ + HCO_3^- \tag{2}$$

A temperature-dependent dissociation constant K can be defined for Eq. (2) (Eq. (2a)):

$$\log K = \frac{a_{H^+} \cdot a_{HCO_3^-}}{a_{H_2CO_3}} = \frac{\gamma_{H^+}[H^+] \cdot \gamma_{HCO_3^-}\left[HCO_3^-\right]}{\gamma_{H_2CO_3}[H_2CO_3]} \tag{2a}$$

where a is activity, [] is concentration, and γ is an activity coefficient. Calculations of log K (Eq. (2a)) using SUPCRT92 [9] show a maximum of dissociation for reaction (2), occurring at about 50 °C above which log K decreases continuously with increasing temperature such that an initially weak acid becomes increasingly weaker at elevated temperature. Thus, at low temperatures, the increased availability of H^+ might be expected to cause higher rates of wallrock hydrolysis. Previous experiments in this laboratory have shown that rhyolite was extensively altered by CO_2-charged water in experiments at 200 °C, but mostly was unreacted at 350 °C [10].

This dissociation of carbonic acid into reactive hydrogen ion and bicarbonate potentially initiates a complex series of reactions with aquifer fluids and formation rocks to fix CO_2 in aqueous and mineral phases. For example, calcite dissolution in response to the increased acidity produced by the dissociation of carbonic acid (Eq. (3)):

$$CaCO_3 + CO_2 + H_2O \rightarrow Ca^{+2} + 2HCO_3^- \tag{3}$$
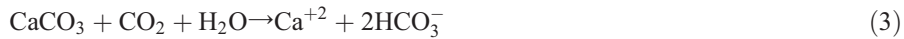
causes an additional mole of CO_2 to be stored as bicarbonate relative to the simple solubility of CO_2 and is an example of the ionic trapping of CO_2. A similar reaction can be written for the dissolution of other carbonates.

Reactions of CO_2-saturated aquifer fluids with arkosic sandstone and available H^+ illustrate the mineral trapping of CO_2 by dissolution of silicates, in particular the anorthitic component of palgioclase (Eq. (4)):

$$2H^+ + CaAl_2Si_2O_8 + H_2O \rightarrow Ca^{+2} + Al_2Si_2O_5(OH)_4 \tag{4}$$

and the subsequent precipitation of calcite (Eq. (5)):

$$Ca^{+2} + HCO_3^- \rightarrow CaCO_3 + H^+ \tag{5}$$

The solubility product ($\log K_{sp}$) of the net reaction (Eq. (6)) decreases with increasing temperature:

$$CaAl_2Si_2O_8 + H_2CO_3 + H_2O = CaCO_3 + Al_2Si_2O_5(OH)_4 \tag{6}$$
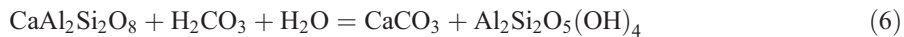
resulting in competing effects of favorable thermodynamics at low temperature versus kinetic considerations that favor reaction rates at elevated temperature.

Reactions involving supercritical CO_2 and carbonic acid with aquifer fluids and formation rocks are thus many and varied, depending on the chemical composition of the fluid and the mineralogy of the rock. In general, CO_2 interaction causes the dissolution of carbonate phases in limestones and the dissolution of silicates and precipitation of carbonates in plagioclase-rich arkosic sandstones. Previous experimental work [11] involving CO_2-saturated brine and arkosic/shale has shown that at least, at 200 °C, some of these reactions are occurring on a measurable time scale. Other workers [12,13] noted only a limited of reaction of CO_2 with pure mineral phases (anorthite and glauconite) or sandstones at 50° and 150 °C and low pressure.

We present here experimental results contrasting the geochemical reactions of supercritical CO_2 with limestone versus a plagioclase-rich arkosic sandstone. We present also the results of CO_2-saturated brine–rock experiments carried out to evaluate the effects of multiphase $H_2O–CO_2$ fluids on mineral equilibria and the potential for CO_2 sequestration in mineral phases within deep-saline aquifers. Experiments were designed to model reactions occurring near the CO_2 injection zone where the aquifer fluid is saturated with excess CO_2 and also at the periphery of the aquifer where the fluid is undersaturated with CO_2.

The goals of experiments involving CO_2 and limestone were twofold: 1) to address a specific brine-disposal problem in a carbonate aquifer located in Paradox Valley, Colorado, a part of the Colorado River desalination project; and 2) to investigate the storage of CO_2 in deep limestone aquifers in general.

2. Experimental methods

2.1. Experimental apparatus

Experimental and analytical procedures followed generally the scheme described in Rosenbauer et al. [14] with some modifications for the injection, sampling, and analysis of CO_2 [15]. Liquid CO_2 was injected into the reaction vessel via syringe pumps (ISCO Corp.) connected to a commercial CO_2 cylinder (Matheson Gas) equipped with a full-length eductor tube for liquid withdrawal. Experiments were carried out in a combination of titanium-lined fixed-volume and flexible-gold reactions cells contained in high-temperature–pressure autoclaves and secured to rotating furnaces [16]. Temperature was maintained by a proportional controller (Love™) and measured with a type K thermocouple calibrated to a platinum resistance temperature detector (RTD). Pressure was measured with dead-weight calibrated analog gauges and digital transducers (Heise). Experiments were carried out at 25° and 120 °C and from 100 to 600 bar.

2.2. Reactants

A shallow ground water brine (PVB) from Paradox Valley, Colorado, and a synthetic mixture of a deep-aquifer brine (PVA), also from Paradox Valley, were reacted with rocks from the Leadville Limestone Formation of Colorado (38% calcite), and arkosic and banded sandstones from Mount Tom in Massachusetts and from Coconio, Arizona, respectively, in the presence and absence of supercritical CO_2. The Mississippian–Leadville Limestone is characterized as a micro- to cryptocrystalline, light-gray limestone with beds of crystalline dolomite (injection well log). The arkose contained, in order of abundance: quartz, plagioclase (oligoclase), potassium feldspar, and kaolinite. The banded sandstone contained: quartz, potassium feldspar, and kaolinite with only minor plagioclase. Both the arkose and banded sandstone contained significant iron (2.9% and 1.5%, respectively). All rocks were ground and sieved between 100 and 200 mesh and washed with distilled water. The PVB is primarily a $NaCl/CaSO_4$ solution also containing large amounts of K and Mg (Table 1) and results from the dissolution of near-surface salt diapirs underlying Paradox Valley in southwest Colorado [17]. The PVA is a synthetic mixture (Table 1) prepared to approximate the composition of the formation water in the Leadville Limestone at Paradox Valley and is primarily a (NaCa)Cl solution. The two brines have similar total salinity but differ in the relative amounts of Ca and SO_4 (Table 1). PVA1 (Table 1) is a synthetic brine with salinity similar to PVA but with Ca, Mg, and K each equal to 1000 ppm. PVA1 was reacted with arkosic sandstone and CO_2 below CO_2 saturation. Starting water/rock ratios were 10/1, typically 200 g of fluid and 20 g of rock. Starting water/liquid CO_2 ratios were ~20/1 in CO_2-saturated experiments.

2.3. Analytical procedures

Periodically, aqueous samples were withdrawn from each experiment and analyzed for total dissolved inorganic carbon species by coulometric titration (Coulometrics™),

Table 1
Composition of Paradox Valley Brines (concentration in mg/L)

Species (mg/L)	Surface (PVB)	Aquifer (PVA)	Aquifer (PVA1)
Na	77,000	70,000	70,000
K	3630	2100	1000
Ca	1187	10,900	1000
Mg	1278	1220	1000
Cl	127,100	132,000	132,000
SO_4	5100	454	454
HCO_3	257	185	100
pH	6.3	5.4	6.5
TDS	215,000	218,000	206,000

PVB is a shallow ground water brine from Paradox Valley, Colorado, PVA is a synthetic solution of a deep-aquifer brine, also from Paradox Valley, PVA1 is a predominantly NaCl solution equivalent in ionic strength to PVB.

dissolved cations by inductively coupled plasma using both atomic emission and mass spectroscopy (ICP-AES, ICP-MS), and dissolved anions by ion chromatograph, except chloride, which was determined by potentiometric titration (chloridometer). Samples were taken hourly or daily near the beginning of each experiment, then at increasingly longer intervals depending on perceived reaction rates and approach to steady-state. Total dissolved CO_2 (C_t) and pH were analyzed immediately after sampling on separate 0.5 ml samples. In situ distribution of carbonate species and pH were calculated from C_t using the computer code SOLMINEQ99 [18] Aliquots for major elements were filtered (0.2μm), diluted, and preserved for batch analyses. The mineralogy of the solids was determined by X-ray diffraction (XRD) and chemistry by total dissolution and ICP-AES (Xral Corporation).

3. Results and discussion

The Bureau of Reclamation has long been investigating ways of disposing a near-surface brine that is contaminating the Dolores River by injection down a deep well (15,000 ft) into the Leadville Limestone aquifer. Previous experiments [17] have shown that direct injection of brine, heated and mixed with formation water, results in serious scaling by $CaSO_4$ precipitates. Thermodynamic modeling predicts that mixing CO_2 with the injecting brine might cause calcite dissolution, increasing the porosity of the formation and hence its capacity for brine disposal with the added bonus of CO_2 removal. Validation of the model would allow the Bureau of Reclamation to use this brine injection scheme as a reservoir for both CO_2 and Paradox Valley brine.

Our experimental results suggest that this is not necessarily the case. In general, we found that the reaction of CO_2 with rocks from limestone aquifers causes carbonates to dissolve and traps CO_2 as an ionic species. But, in the particular case of simulated co-injection of supercritical CO_2 with brine into limestone, neither the geochemical reactions nor the rock porosity were significantly affected by the presence of supercritical CO_2 except for some initial dissolution of calcite in the presence of supercritical CO_2. Results

from the interaction of supercritical CO_2 with arkose and brine support the hypothesis that CO_2 can be sequestered in mineral phases and that this process occurs on measurable timescales.

3.1. Reactions in limestone

3.1.1. Limestone–PVB reactions (ionic trapping)

At 25° and 120 °C, the reaction of CO_2-saturated PVB with limestone rocks is characterized by a pressure-dependent enhanced solubility of CO_2 relative to the solubility of CO_2 in PVB alone. (Fig. 1). This increase in the solubility of CO_2 is due to the apparent rapid dissolution of calcite in response to the increased acidity produced by the dissociation of carbonic acid (Eq. (3), above), in which CO_2 is stored as bicarbonate and is an example of the ionic trapping of CO_2. Calcite has a retrograde with respect to temperature solubility and is, therefore, less soluble and less efficient at ionic trapping of CO_2 at elevated temperature. Experimental results show that the solubility is enhanced 8.8% at 25 °C and 5.7% at 120 °C and 300 bar, compared to the solubility in the brine itself.

For comparison, at 25 °C, there is a significant 4% increase in the solubility of CO_2 in the natural brine alone relative to an equivalent ionic strength NaCl solution [6] due to the presence of divalent cations in the brine that likely form bicarbonate complexes. The extent of this offset between the solubility in PVB and NaCl decreases with increasing temperature and becomes negligible near 50 °C [6].

The reaction of PVB with carbonate rocks from the Leadville Limestone Formation in the absence of CO_2 at 120 °C and 300 bar results in a complex pattern of change in the fluid chemistry (Fig. 2a). Temporal changes are illustrated in Fig. 2a (from earlier work in this laboratory [17]) by changes in dissolved Ca, Mg, and SO_4. Simultaneous and competing reactions first remove then add Ca to solution, while Mg and SO_4 continuously decrease. Initially, Ca and SO_4 decrease sharply in near equimolar amounts
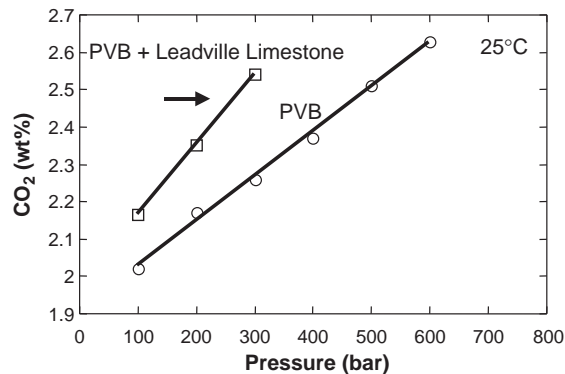

Fig. 1. The solubility of CO_2 in Paradox Valley Brine (PVB) in the presence (open square symbols) and absence (open circles) of rocks from the Leadville Limestone (LVL) at 25 °C. Curves are linear regressions of the data points.
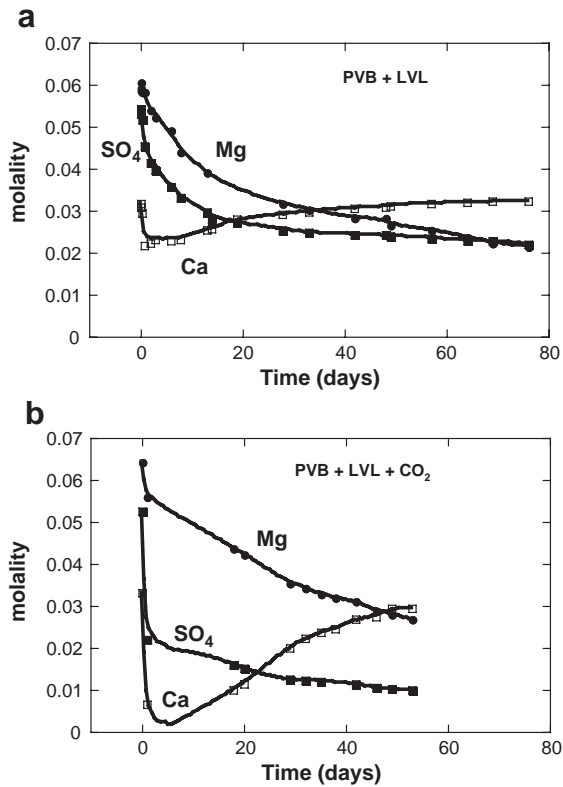
Fig. 2. Changes in concentration with time of dissolved components when PVB is reacted with rocks from the Leadville Limestone (LVL) at 120 °C, and 300 bar, both in the presence (b) and absence of supercritical CO_2 (a). Water–rock ratio=10; CO_2–water ratio=20. The experimental data are shown by symbols (solid circles=Mg; solid squares=SO_4; open squares=Ca). Curves are smooth fits through the data.

consistent with the formation of anhydrite (Eq. (7)). Anhydrite was identified in the reactions products:

$$Ca^{+2} + SO_4^{-2} \leftrightarrow CaSO_4 \tag{7}$$

The removal of Mg and the addition of Ca to solution is caused by the conversion of calcite to dolomite (Eq. (8)):

$$Mg^{+2} + 2CaCO_3(\text{calcite}) = CaMg(CO_3)_2(\text{dolomite}) + Ca^{+2} \tag{8}$$
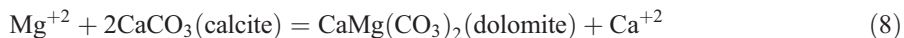
Calculations using SOLMINEQ99 [18] of saturation indices (SI) of individual minerals indicate that the initial fluid is close to equilibrium with anhydrite, calcite, and a disordered dolomite (Table 2). If CO_2 is added to the simulated system, anhydrite remains saturated but the carbonates become undersaturated (Table 2). Increasing the temperature to 120 °C causes anhydrite initially to become supersaturated (SI=0.6; Table 2) but reduces to near saturation at the end of the experiment. Based on mass balance calculations for Mg, Ca,

Table 2
Modeled mineral saturation indices for PVB at 300 bar calculated using the geochemical program SOLMINEQ

Phase	Log (Q_{IAP}/K_{SP})		
	25 °C	25 °C, CO_2-saturated	120 °C, CO_2-saturated
Anhydrite	−0.02	−0.03	+0.60
Calcite	−0.12	−2.7	−2.1
Dolomite	+1.21	−3.8	−2.2
Dolomite (disordered)	−0.33	−5.4	−3.2

PVB is a shallow ground water brine from Paradox Valley, Colorado. Q_{IAP}=ion activity product; K_{SP}=solubility product.

and SO_4, 25% of the original calcite dissolved or was dolomitized. Net molar volume changes of reactions (4) and (5) result in porosity decrease of 5% in the rock.

Remarkably, the overall pattern of compositional change of the fluid with the addition CO_2 (Fig. 2b) to the injection stream was almost identical to the system without added CO_2 except for a calculated in situ pH between 4.1 and 4.3 in the presence of CO_2, contrasted with a pH of 6.7 in the absence of CO_2. The reactions in both experiments are dominated by the precipitation of anhydrite, dissolution of calcite, and dolomitization of the limestone. Overall porosity changes are also similar. However, in the very early stages (2 days) of the experiment with added CO_2 (Fig. 3), dissolved Ca and Mg increase sharply, accompanied by only a minor decrease in SO_4, likely due to the dissolution of calcite and dolomite and precipitation of some anhydrite. Based on mass balance calculations for Ca, Mg, and SO_4 and molar volumes for calcite, dolomite, and anhydrite, net porosity change is very favorable at −15%. The combination of CO_2 co-injection with other mitigation strategies such as dilution with Dolores River water [17] or the use of nano-filtration membranes [19] might therefore help alleviate some of the well-bore scale and formation-
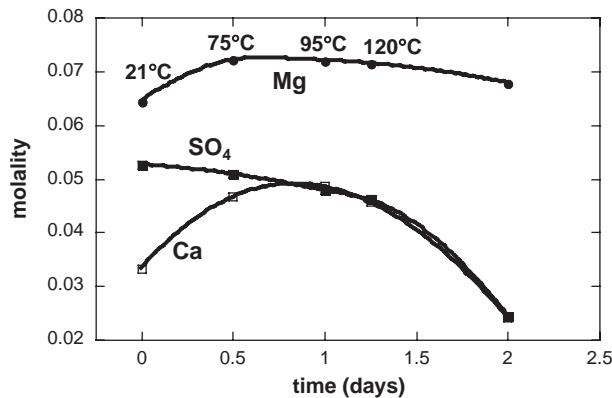

Fig. 3. Expanded view of Fig. 2b, showing the first 2 days of changes in concentration with time of dissolved components when PVB is heated and reacted with rocks from the Leadville Limestone at 120 °C and 300 bar, in the presence of a CO_2 phase. Water–rock ratio=10; liquid CO_2–water ratio=20. The experimental data are shown by symbols (solid circles=Mg; solid squares=SO_4; open squares=Ca). Curves are smooth fits through the data. The experiment was sampled at the indicated temperatures during heating to 120 °C.

plugging problems near the injection zone in Paradox Valley as well as provide a repository for CO_2.

3.1.2. Limestone–PVA reactions

At 120 °C and 300 bar pressure, and in the presence of a separate supercritical CO_2 phase, the reaction of PVA with rocks from the Leadville Limestone Formation is characterized by compositional changes in the fluid caused by calcite and dolomite dissolution and anhydrite precipitation. The pattern of fluid changes is illustrated in Fig. 4a–c by temporal changes in Ca, Mg, and SO_4 concentrations, respectively. Calcium increases rapidly to near steady-state concentration within 3 days (Fig. 4a). Magnesium ion concentration increases initially, then reverses and continuously decreases (Fig. 4b). And the relatively small amount of initial SO_4 rapidly decreases (Fig. 4c) due to anhydrite precipitation. Increases in Ca and Mg are caused by calcite and dolomite dissolution; significantly more calcite dissolved (3.7 mM) than dolomite (0.8 mM). The decrease in Mg lags the increase in Ca, indicating that Mg is precipitating in some other phase than dolomite such as smectite or magnesite. Again, the experimental results are in agreement with calculated saturation indices. Unreacted PVA at 120 °C is initially in equilibrium with anhydrite, calcite, and disordered dolomite (Table 3). The addition of CO_2 to the system causes only the carbonates to become under-saturated. But in the experiment, the increase in Ca from the dissolution of calcite causes SO_4 to precipitate as anhydrite (0.4 mM). These results, combined with the results from the reaction of PVB with limestone at elevated temperature, show that anhydrite precipitation is kinetically rapid and may lead to scaling and a reduction in formation porosity when CO_2 is injected into a deep aquifer. Any process leading to a significant increase in dissolved Ca or SO_4 could result in supersaturation with respect to anhydrite. For example, CO_2 injection itself increases dissolved Ca by the dissolution of Ca-bearing carbonates, and dissolved SO_4 would be increased by the co-injection and solution of SO_2 [20,21], a natural waste product in many power plant flue gases along with CO_2. SO_2 rapidly reacts with water to produce mostly SO_4 and minor reduced sulfur-bearing species such as sulfide, sulfite, and thiosulfate (Eq. (9), for example):

$$4SO_2(g) + 4H_2O = 3H_2SO_4 + H_2S \tag{9}$$

Compared to the reactions involving CO_2-saturated PVB and limestone, changes due to reactions involving CO_2-saturated PVA are less, mostly due to the lower concentration of dissolved SO_4 and result in a net porosity increase of 2.6%.

3.1.3. PVA–CO_2 reactions

The reaction of supercritical CO_2 with PVA in the absence of limestone is characterized by a small increase in TDS illustrated by temporal changes in dissolved Ca (Fig. 4a) and Mg (Fig. 4b). In the absence of any apparent source, Ca and Mg each increases ~2%. These changes are caused by the solubility of water in the CO_2 phase and the transfer of pure water from the brine phase to the CO_2 phase. In a separate experiment at similar conditions designed to measure the solubility of CO_2 in NaCl solutions, we measured ~1.5% water in the CO_2 phase. The solubility of H_2O in supercritical CO_2 is temperature- and pressure-dependent [6,8] and has been noted by others [11] who refer to the
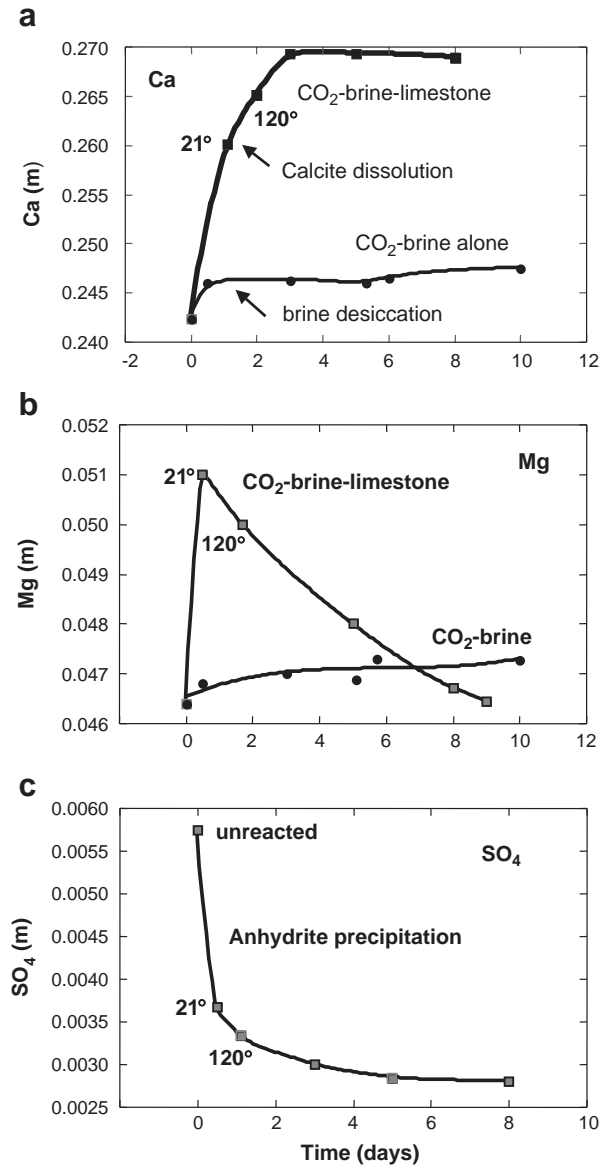
Fig. 4. (a–c) Changes in concentration with time of dissolved components when CO_2-saturated PVA is heated in the presence (squares) and absence (circles) of rocks from the Leadville Limestone at 120 °C and 300 bar. Water–rock ratio=10; liquid CO_2–water ratio=20. Symbols represent samples and experimental data. Curves are smooth fits through the experimental data. Changes in concentrations are shown at 21 °C for 1 day and at 120 °C for the remainder of each experiment.

Table 3
Modeled mineral saturation indicies for PVA at 125 °C and 300 bar, calculated using the geochemical program SOLMINEQ

Phase	Log (Q_{IAP}/K_{SP})		
	PVA alone	PVA saturated with CO_2	PVA saturated with CO_2 and calcite
Anhydrite	+0.15	+0.15	+0.04
Calcite	−0.05	−1.7	+0.01
Dolomite	+0.76	−2.5	+0.82
Dolomite (disordered)	−0.11	−3.4	−0.06

PVA is a synthetic solution of a deep-aquifer brine from Paradox Valley, Colorado. Q_{IAP}=ion activity product; K_{SP}=solubility product.

phenomenon as desiccation of the brine. The solubility of H_2O in supercritical CO_2 generally increases with increasing temperature and pressure[5]. Aquifer systems near saturation with mineral phases would be susceptible to precipitation reactions and porosity reduction by this process.

3.2. Reactions in arkosic sandstones (mineral trapping)

3.2.1. Sandstone–PVA reactions

Interactions of arkosic and of iron-rich banded sandstones with PVA are characterized by large changes in elemental abundances, enhanced CO_2 solubility, and desiccation of the brines. Prior to injection of liquid CO_2, changes occurred in dissolved Ca, Mg, K, and Na during brine interaction with minerals. The arkose–PVA experiment was of longer duration and exhibited larger fluid compositional changes probably due to the more complex mineralogy of the arkose compared to the banded sandstone. The direction of change was generally similar in both the banded sandstone and arkose experiments, but the fluid composition reached steady-state sooner in the experiment with banded sandstone than the experiment with arkose (Fig. 5a–c). Dissolved Ca decreased slightly at first then reversed and increased continuously with arkose but decreased only slightly and remained constant thereafter with the banded sandstone. Mg and K decreased and Na first increased then decreased in both experiments, likely caused by equilibration with clays and K-feldspar.

Upon injection of liquid CO_2, total dissolved solids (TDS), including Cl, increased sharply in both experiments due to the transfer of H_2O from the brine to the CO_2 phase (Fig. 6). Kaszuba et al. [11] noted that in similar experiments dissolved Cl increased by 25% after CO_2 was injected into a saline brine, pre-equilibrated with arkose and shale at 200 °C and 200 bar. Highly saline aquifers near saturation with NaCl would precipitate halite under these conditions.

Similar to the results of Kaszuba et al. [11], increases in dissolved elemental concentrations in the present experiments were not proportional with dissolved Cl (Table 4). In our experiments, changes ranged from 2% for Cl to 12% for Mg immediately after injection of CO_2 into the brine, indicative of a variety of fluid–rock interactions. These changes were less than those observed by Kaszuba et al., likely due
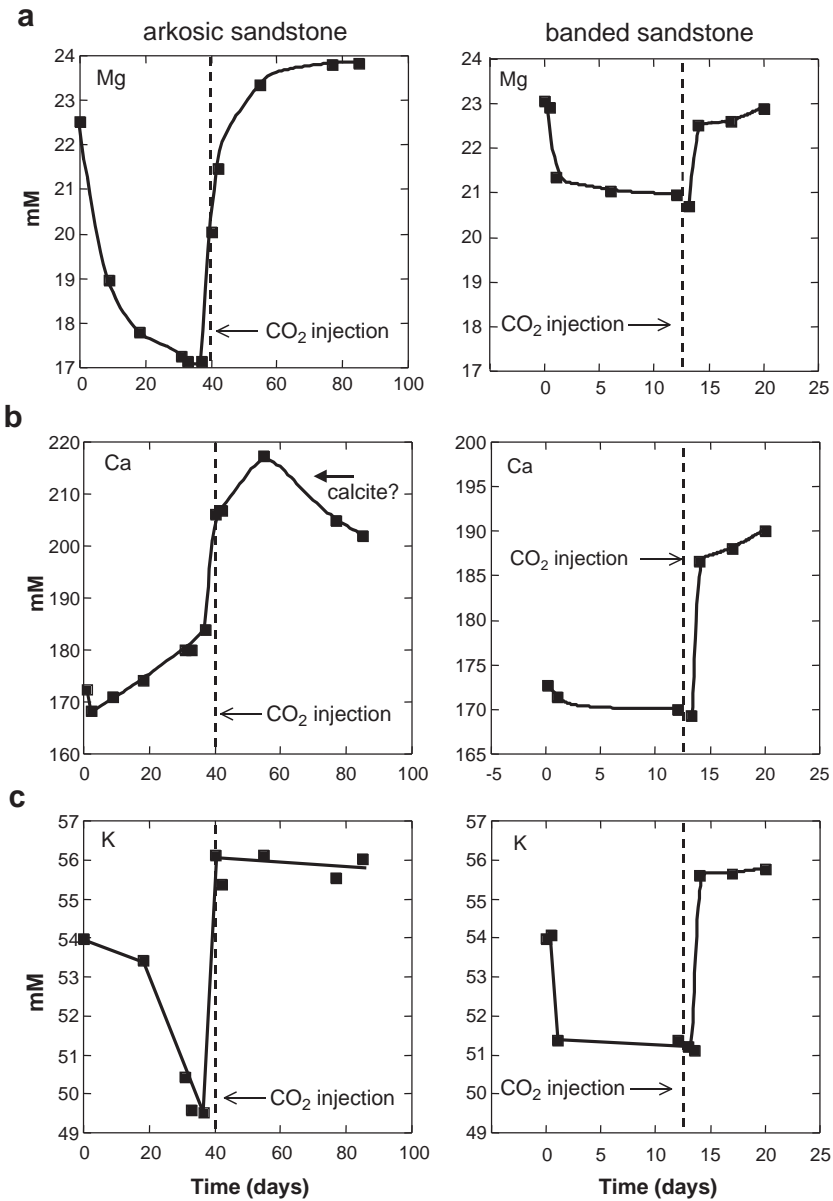
Fig. 5. Changes in concentration with time of dissolved components before and after injection of liquid CO_2 when PVA brine is reacted with arkosic (left) and banded (right) sandstones at 120 °C and 300 bar. Water–rock ratio=10; liquid CO_2–water ratio=20. Symbols represent samples and experimental data. Curves are smooth fits through the experimental data.
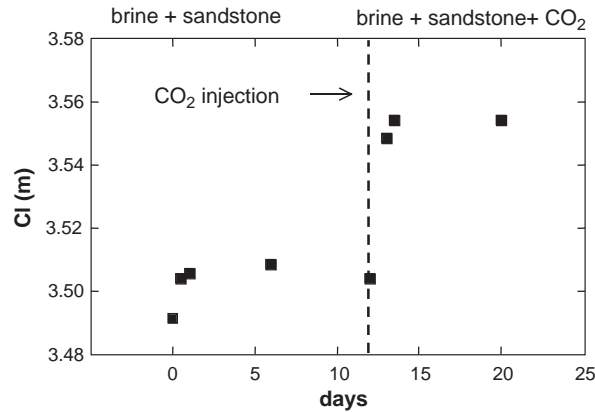
Fig. 6. Changes in concentration with time of dissolved Cl before and after injection of liquid CO_2 when PVA brine is reacted with arkosic sandstone at 120 °C and 300 bar. Water–rock ratio=10; liquid CO_2–water ratio=20. Symbols represent samples and experimental data.

to the difference in temperature, but the results indicate that significant water–rock interaction occurred even at moderately low temperature (120 °C). The decrease of dissolved Ca time after injection of CO_2 into PVA equilibrated with arkose likely indicates fixation of CO_2 as calcite. Significant metals were released to solution, in particular Fe from both the arkose and banded sandstones (Fig. 7), leading to the possibility of siderite precipitation.

3.2.2. Arkosic sandstone CO_2-unsaturated PVA1 reactions

Arkose was reacted with PVA1, undersaturated with CO_2 to model the periphery of an aquifer where its area and reacting volume is greatest and where the buffering capacity of the rock is highest relative to the concentration of H^+. In the absence of a separate CO_2 liquid-phase reservoir, the acidity produced by the dissociation of carbonic acid is more easily neutralized by minerals in the solid phase, resulting in a higher pH,

Table 4
Initial change in dissolved chemistry after injection of CO_2 into brines initially equilibrated with sandstones at 300 bar from this study compared to Kaszuba et al. [11]

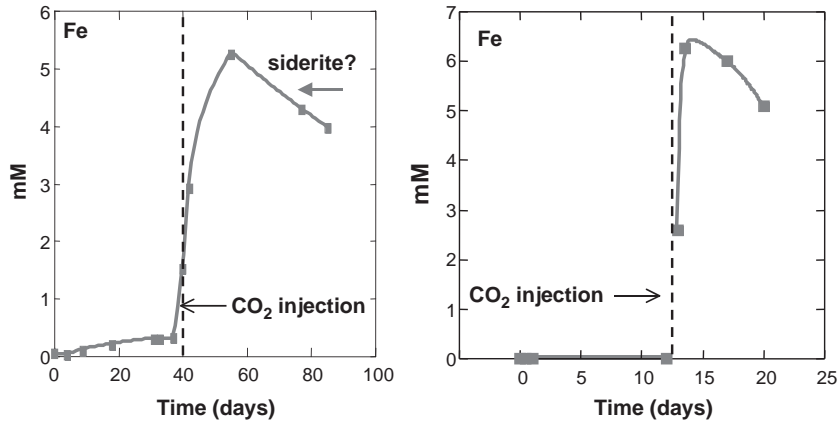| Component	% Change after CO_2 injection		
	This study, banded, 120 °C	This study, arkose, 120 °C	Kaszuba et al. [11], arkose/shale, 200 °C
Ca	12	12	50
Mg	10	17	38
Na	16	22	19
K	8.8	13	36
Cl	2	2.1	25
Fe (mM)	6.0	4.3	4.6
Mn (mM)	0.12	1.3	0.12

Fig. 7. Dissolved Fe concentrations in PVA brine reacted with arkosic (left) and banded (right) sandstones at 120 °C and 300 bar in the presence of supercritical CO_2. Symbols represent samples and experimental data. Curves are smooth fits through the experimental data.

precipitation of carbonate phases, and sequestration of CO_2. We used a modeled simulation (Fig. 8) of chemical and mineralogical changes that occur as a function of the amount of CO_2 added to the brine (PVA1) arkose system as a guide for determining the
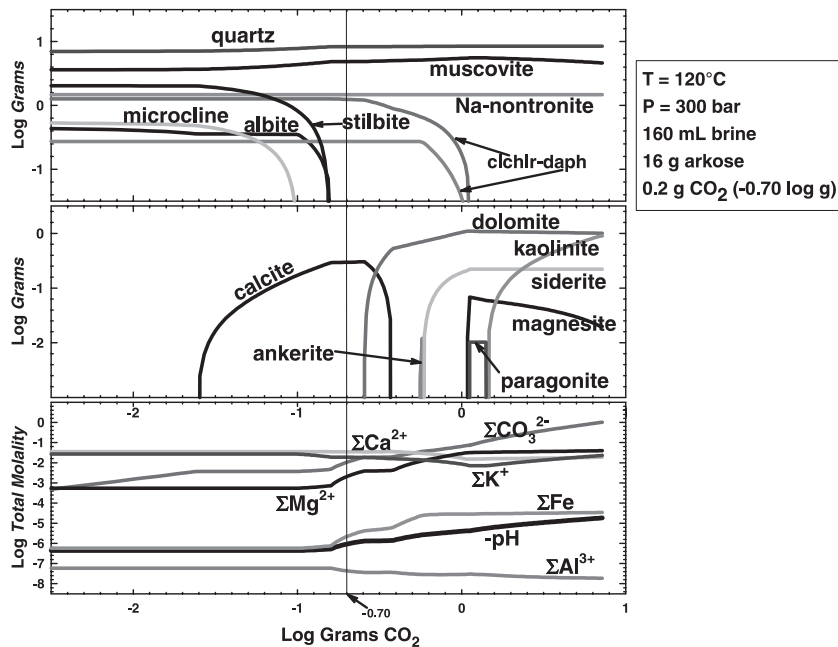
Fig. 8. Modeled mineralogical and compositional changes as a function of CO_2 added to arkose and brine. Optimal experimental conditions, indicated by the vertical line at log CO_2 (g)=−0.7, were chosen near the maximum in calcite precipitation and where albite (anorthite) and stilbite reach maximum dissolution. Calculations performed using the geochemical program CHILLER.
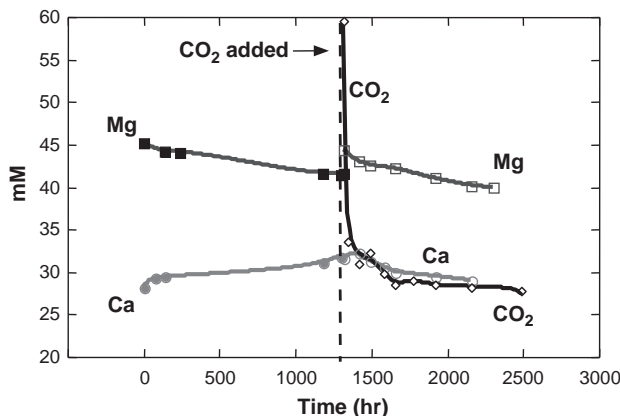
Fig. 9. Changes in concentration with time of dissolved components before and after injection of CO_2 when PVA1 brine is reacted with arkosic sandstone at 120 °C and 300 bar. Water–rock ratio=10; initial total dissolved CO_2=0.22%. Symbols represent samples and experimental data. Curves are smooth fits through the experimental data.

experimental conditions, using the geochemical program CHILLER [22,23]. In the experiment, we added 0.2 g of CO_2 to maximize the amount of calcite predicted to form (Fig. 8) and where albite (anorthite) and stilbite (altered anorthite) are projected to completely dissolve.

Prior to adding CO_2 to the experiment, the arkose was reacted with PVA1; Ca increased and Mg decreased to near steady-state (Fig. 9). After CO_2 injection, CO_2 dropped rapidly due probably to an initial heterogeneous dissolution of CO_2 because the decrease was not accompanied by other solution changes that would indicate carbonate precipitation. That the initial sampling after CO_2 injection occurred before all the CO_2 dissolved is consistent with the upward spike in dissolved Mg and
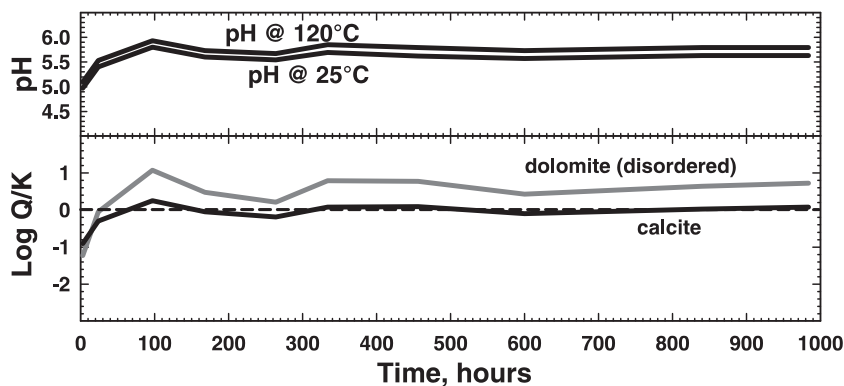

Fig. 10. Modeled maximum pseudo-saturation indices for dolomite, magnesite, and calcite when arkose is reacted with CO_2 (22%) at 120 °C and 300 bar. In situ pH and saturation indices were calculated with the geochemical program SOLVEQ using partially degassed 25 °C pH measurements and total carbon.

dewatering of the brine. It is also possible that the decrease in CO_2 was simply due to unmixed CO_2 post-injection, but CO_2 injection procedures are designed to minimize this artifact. Subsequent to the rapid decrease in CO_2, both Ca and CO_2 decrease slightly but continuously in almost equi-molar amounts, consistent with calcite precipitation (Fig. 9). Mg also decreases continuously after spiking upward following the injection of CO_2. These results are consistent with calculated pseudo-saturation indices for calcite (Fig. 10), which are based on partially out-gassed pH measurements at 25 °C, using the geochemical program SOLVEQ [22,23], and even at the relatively low temperature of 120 °C, these reactions can occur on measurable time scales.

4. Conclusions

Experimental results are generally consistent with theoretical calculations. CO_2-saturated brine–limestone reactions are characterized by compositional, mineralogical, and porosity changes that are dependent on initial brine composition, especially on the content of dissolved sulfate, as are the changes in aquifer porosity. The direction and magnitude of porosity changes are a function of geochemical reactions involving dolomitization of calcite and the precipitation of anhydrite. The dissolution of calcite and dolomitization increases porosity; the precipitation of anhydrite decreases porosity. Based on favorable initial porosity changes, the combination of CO_2 co-injection with other mitigation strategies might help alleviate some of the well-bore scale and formation-plugging problems near the injection zone in Paradox Valley as well as provide a repository for CO_2.

Although the solubility of CO_2 is enhanced in the presence of both limestone and sandstone rocks, storage of CO_2 in limestone formations is limited to ionic and hydrodynamic trapping; albeit the kinetics of these geochemical reactions is rapid.

Reactions between CO_2-saturated and unsaturated brines and arkosic sandstones are characterized by desiccation of the brine and changes in the chemical composition of the brine, suggesting fixation and sequestration of CO_2 in mineral phases especially at conditions that model the periphery of an aquifer. These reactions are occurring on measurable but kinetically slow time scales at 120 °C.

The experimental results suggest that it is inadvisable to either co-inject SO_2 into high-Ca brines due to likely anhydrite precipitation or inject CO_2 into brines near saturation with mineral phases due to desiccation effects of the brine-promoting precipitation reactions.

References

[1] T.B. Johnansson, R.H. Williams, H. Ishitani, J.A. Edmonds, Energy Policy 24 (10–11) (1996) 985–1003.
[2] R.G. Bruant Jr., M.A. Celia, A.J. Guswa, C.A. Peters, Environ. Sci. Technol. 36 (11) (2002) 240–245.
[3] T.F. Stocker, A. Schmittner, Nature 388 (1997) 862–865.
[4] M.R. Allen, P.A. Stott, J.F.B. Mitchell, R. Schnur, T.L. Delworth, Nature 407 (2000) 617–620.
[5] T.N. Palmer, J. Räisänen, Nature 415 (2002) 512–514.
[6] R.J. Rosenbauer, T. Koksalan, GSA Abstracts with Programs, Annual Meeting, Denver, CO, vol. 135 (2), 2002 (October 27–30), p. 304.
[7] Z. Duan, R. Sun, Geochim. Cosmochim. Acta 6 (20) (1996) 3859–3867.
[8] S. Takenouchi, G.C. Kennedy, Am. J. Sci. 262 (1964) 1055–1074.
[9] J.W. Johnson, E. Oelkers, H.C. Helgeson, Comput. Geosci. 18 (1992) 899–947.
[10] J.L. Bischoff, R.J. Rosenbauer, Chem. Geol. 193 (2003) 257–271.
[11] J.P. Kaszuba, D.R. Janecky, M.G. Snow, Appl. Geochem. 18 (7) (2003) 1065–1080.
[12] B.M. Sass, M.H. Engelhard, P. Berman, C. Byrer, J. Energy Environ. Res. 2 (2002) 23–31.
[13] N. Gupta, B. Sass, J. Ickes, Tech Prog. Rep. Prepared for C. Byrer (DOE) (2000) 18 pp.
[14] R.J. Rosenbauer, J.L. Bischoff, A.S. Radke, Econ. Geol. 78 (1983) 1701–1710.
[15] R.J. Rosenbauer, T. Lorenson, Eos. Trans. AGU, Spring Meet. Suppl. Abstracts, Boston, MA, March 29–April 2, 2001, H31C-15.
[16] R.J. Rosenbauer, J.L. Bischoff, J. Potter, Am. Mineral. 78 (1993) 1286–1289.
[17] R.J. Rosenbauer, J.L. Bischoff, Y. Kharaka, Appl. Geochem. 7 (1992) 273–286.
[18] Y.K. Kharaka, W.D. Gunter, P.K. Aggarwal, E.H. Perkins, J.D. Debraal, U.S. Geol. Surv., Water Resour. Investig. Rep. (1988) 88–427.
[19] Y.K. Kharaka, G. Ambats, J.J. Thorsden, R.A. Davis, Water Resour. Res. 33 (5) (1997) 1013–1020.
[20] R.J. Rosenbauer, J. Koksalan, Extended Abstracts, the 227th ACS National Meeting, Anaheim, CA, March 28–April 1, 2004.
[21] J. Palandri, R.J. Rosenbauer, J. Palandri, NETL, Extended abstracts, Third Annual Conference on Carbon Capture and Sequestration, May 2–6, 2004.
[22] M.H. Reed, Geochim. Cosmochim. Acta 46 (1982) 513–528.
[23] M.H. Reed, in: J. Richards, P. Larson (Eds.), Techniques in Hydrothermal Ore Deposits Geology, Economic Geology, 1998, pp. 109–124.